Int. J. Solids Structures Vol. 23, No. 12, pp. 1657–1664, 1987
Printed in Great Britain.

0020-7683/87 $3.00+.00

ELASTIC ANALYSIS OF SOME PUNCH PROBLEMS FOR A LAYERED MEDIUM

R. B. KING
IBM Almaden Research Center, 650 Harry Road, San Jose, CA 95120-6099, U.S.A.

(*Received* 18 *February* 1987; *in revised form* 15 *April* 1987)

Abstract—The problems of flat-ended cylindrical, quadrilateral, and triangular punches indenting a layered isotropic elastic half-space are considered. The former two are analyzed using a basis function technique, while the latter problem is analyzed via a singular integral equation. Solutions are obtained numerically. Load–deflection relations are obtained for a series of values of the ratio of Young's modulus in the layer and substrate, and for a variety of punch sizes. These solutions provide an accurate basis for the estimation of Young's modulus of thin films from the initial unloading compliance observed in indentation tests, and are specifically relevant to axisymmetric, Vicker's, and triangular indenters. The results should also be of interest in foundation engineering.

1. INTRODUCTION

Indentation tests are a promising means of obtaining mechanical property information for thin films, as is reviewed in detail in Ref.[1]. Loubet *et al.*[2] suggested that Young's modulus can be inferred from an elastic analysis of the initial slope of the unloading portion of a plot of indentation load as a function of penetration depth, shown schematically in Fig. 1. This is because even though the specimen has undergone elastic–plastic deformation during loading, the initial unloading is an elastic event. Assuming that the contact area remains constant during initial unloading, an approximate elastic solution is obtained by analyzing a flat-ended punch the area of which in contact with the specimen is equal to the projected area of the actual punch. Both the assumptions that initial unloading is elastic and that the contact area remains constant during initial unloading are supported empirically by the fact that the initial unloading portion of the load vs depth curve is linear: both plasticity and varying contact area are non-linear phenomena. A flat-ended punch solution exists for a circular punch contacting a half-space[3], but not for quadrilateral or triangular punch shapes. The latter two are more typical of what is used experimentally.

The solution for a circular punch indenting a half-space yields

$$S_0 \equiv \mathrm{d}P/\mathrm{d}h = 2r_0E_r \tag{1}$$

where

$$1/E_r = (1-\nu_0^2)/E_0 + (1-\nu^2)/E_s$$

P is the load, h the penetration depth, E_0, ν_0 and E_s, ν are Young's modulus and Poisson's ratio for the indenter and substrate (half-space) respectively, and r_0 is the radius of the punch. Loubet *et al.*[2] and Doerner and Nix[1] suggested using the circular punch solution and determining r_0 by equating the area of the cylindrical punch to the actual projected area. If E_0, ν_0, and ν are known, then E_s can be inferred from the measured value of S_0 as shown in Fig. 1. This estimation will become increasingly inaccurate when applied to thin films as the ratio of punch size to film thickness, t, increases, because of the increasing importance of the elasticity of the substrate material underlying the film. It was suggested in Ref.[1] that the influence of the substrate could be accounted for by replacing E_r in eqn (1) with

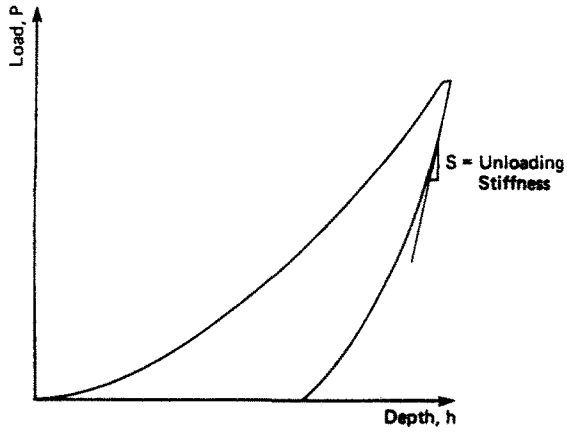

Fig. 1. Load as a function of penetration depth in an indentation test.

$$E_r = \{(1-\nu_f^2)/E_f(1-e^{-\alpha t/a})+(1-\nu_s^2)/E_s\, e^{-\alpha t/a}+(1-\nu_0^2)/E_0\}^{-1} \tag{2}$$

where the subscripts s and f refer to the substrate and film properties, a is the square root of the projected contact area, and α is an unknown parameter. In Ref. [1] eqn (2) was presented based on the indentation depth h. The relation between h and a is punch geometry dependent, so a will be used here instead. An empirically determined value of α was presented in Ref. [1] based on measurements of tungsten films on silicon substrates.

The solutions presented in this paper form the basis for a more accurate estimation of Young's modulus from indentation tests. Solutions for a layered half-space are presented for circular, square, and triangular punches. The theoretical background is described in Section 2. Results are presented in Section 3 for circular, square, and triangular punches. The latter two solutions will provide more accurate results for Vicker's and triangular punches than the use of an "effective" circular solution for these geometries, as is illustrated.

Curves showing the influence of substrate elasticity on unloading compliance are presented. It is shown that eqn (2) is an excellent functional form for describing the influence of the substrate, and theoretically determined values of α are given.

2. THEORETICAL BACKGROUND

A theoretical procedure for analyzing elastic normal contact problems for layered media was presented by Chen and Engel[4] and used by the author to study sliding contact[5]. For a flat-ended punch, the boundary condition at the interface between punch and half-space is

$$w(x, y)+w_0(x, y) = W \tag{3}$$

where W is a prescribed displacement remotely applied to the indenter. An efficient numerical technique is to satisfy eqn (3) in a least squares sense by minimizing

$$\int_A (W-w-w_0)^2\, dA. \tag{4}$$

Expanding the unknown pressure distribution at the interface in terms of a series of basis functions

$$p(x, y) = \sum_{i=1}^{N} b_i p_i(x, y)$$

denoting the value of $(w+w_0)$ corresponding to each basis function acting alone as w_i, and substituting in eqn (4) results in the normal equations

$$[K]\mathbf{b} = \mathbf{f} \tag{5}$$

where

$$K_{ij} \equiv \int_A w_i w_j \, dA \qquad \text{and} \qquad f_i \equiv \int_A w_i W \, dA.$$

A small number of basis functions was found to be needed in practice to yield good accuracy, and ten-point Gauss quadrature[6] was sufficient for carrying out the integrations. The choice of basis functions used was $p_1 = 1/\sqrt{(r_0^2 - r^2)}$, $p_i = \cos((i-1)(\pi/2)(r/r_0))$, $i = 2\ldots$ for the axisymmetric case where r_0 is the radius of the punch. The first basis function is suggested by the exact solution to a circular punch encountering a half-space, while the remainder represent a complete set that can represent any arbitrary perturbation to the half-space solution caused by the presence of the layer. For arbitrary quadrilateral punches (e.g. the Knoop indenter) the indenter is first mapped to a square extending from $(x', y') = (-1, -1)$ to $(x', y') = (1, 1)$ and the numerical integration is carried out in the transformed space with the determinant of the Jacobian of the transformation appearing in the integrand. This mapping would be necessary to model non-rectangular geometries such as the Knoop indenter but is not needed for indenters such as the Vicker's. The pressure is expanded in a series of functions in x' multiplied by the same series in y', with the first function the same as in the axisymmetric case and the higher order functions given by $p_2 = 1$, and $p_i = \cos((i-2)(\pi r/2r_0))$, i odd; $p_i = \sin((i-1)(\pi r/2r_0))$, i even; $i = 3\ldots$. The asymmetric (sin) functions are omitted for rectangular punches.

It remains to evaluate the w_i for a layered medium. This can be done using the theory of Burmister for a single layer on a half-space[7] or of Chen for multiple layers[8]. Using Burmister's theory, the solution for a point load located a distance r from a field point is

$$G(r) = \int_0^\infty \left[\frac{1+4B_k\omega t e_2 - B_k B_l e_4}{1-e_2(B_l+B_k+4B_k(\omega t)^2)+4B_k B_l e_4}\right] J_0(\omega r)\, d\omega \tag{6}$$

where $e_2 \equiv e^{-2\omega t}$, $e_4 \equiv e_2^2$, and B_k, B_l, B_n are constants presented in Ref. [7] depending on E_s, ν_s, E_f, ν_f. The term in brackets quickly approaches unity for large ω. Letting g be the integrand in eqn (6)

$$\int_{\omega_{max}}^\infty g \, d\omega$$

is given by

$$B_{max}/R\left\{1 - \omega_{max} r J_0 + \frac{\pi}{2}\omega_{max} r(J_0 H_1 - J_1 H_0)\right\}$$

where B_{max} is the term in brackets in eqn (6) evaluated at ω_{max} and J_0, J_1, H_0, H_1 are asymptotic forms for the Bessel and Hankel functions evaluated at $\omega_{max} r$. Equation (6) can then be efficiently evaluated by numerically integrating up to ω_{max} and adding on the analytic expression for high frequencies. In practice, $\omega_{max} t = 20$ was found to be sufficient.

After tabulating $G(r)$, the w_i are evaluated by superposition

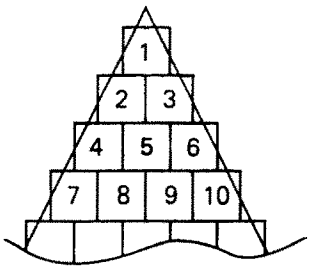

Fig. 2. Quadrature cell numbering in numerical solution of integral equation for triangular punches.

$$w_i(x, y) = \int_A p_i(\xi, \eta) G(r)\, dA$$

where $r = \sqrt{((x-\xi)^2+(y-\eta)^2)}$. The integral is evaluated numerically using rectangular-rule quadrature[9]. Care must be taken when r approaches zero. There, an asymptotic expression is used for $G(r)$ and integrated in closed form as presented in the appendix. For the axisymmetric case an alternate solution for w_i may be obtained by superposition in the frequency domain as described in Ref. [5]. The two approaches gave the same result for w_i within 0.1%, giving confidence in the numerical procedure.

For the case of a triangular punch, the basis function approach was abandoned because it was not obvious what set of functions would quickly converge. Instead, an integral equation approach was used. Expressing $(w+w_0)$ in terms of $G(r)$ and substituting in the boundary condition, eqn (3), results in

$$W = \int_A p(\xi, \eta) G(r)\, dA \tag{7}$$

which is a singular integral equation for the unknown pressure $p(x, y)$. This is evaluated by the rectangular rule, resulting in the discretized equations

$$\sum_{j=1}^{N} G_{ij} p_j = W \tag{8}$$

where N is the number of quadrature cells, and the convention used in numbering the ith cell is shown in Fig. 2. As in the basis function approach, an analytical expression for

$$\int_{A_i} G(r)\, dA$$

is used for small r. Equation (8) is a linear system that is solved for the p_i. It is a much larger system than the equivalent system for the basis function case, eqn (5), which is the disadvantage of the integral equation approach. To get adequate accuracy (error of less than 0.5%) in the calculation of load, it was found that approximately 200 integration cells were needed, requiring about 10 CPU seconds for the evaluation of eqn (8) on an IBM 3081. The load is evaluated after determining the pressure distribution by numerical quadrature over the punch area.

3. RESULTS AND DISCUSSION

Solutions for each of the geometries studied were first calculated for the half-space only. The results may be put in the form

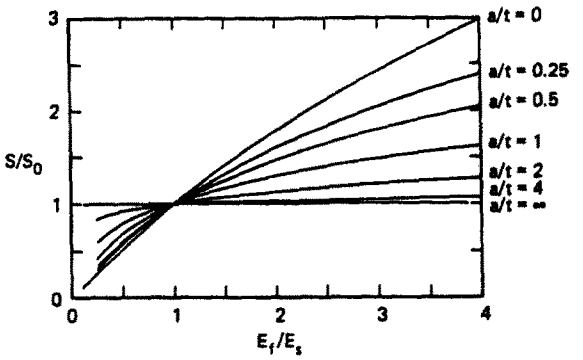

Fig. 3. Normalized unloading stiffness vs normalized film stiffness for a circular punch.

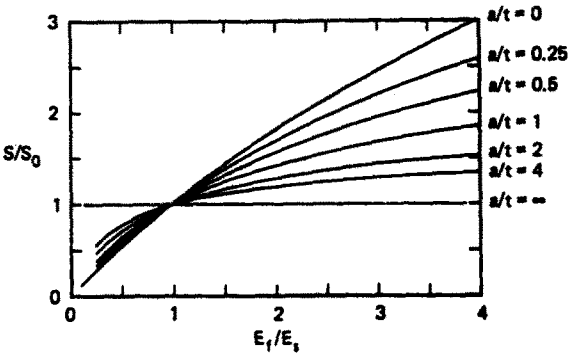

Fig. 4. Normalized unloading stiffness vs normalized film stiffness for a square punch.

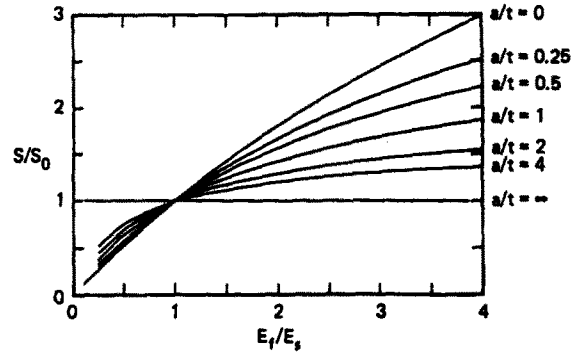

Fig. 5. Normalized unloading stiffness vs normalized film stiffness for a triangular punch.

$$S_0 = \beta E_r \sqrt{A} \tag{9}$$

where A is the contact area, and β is a numerical factor the value of which is given by

circle, $\beta = 1.129$;
square, $\beta = 1.142$;
triangle, $\beta = 1.167$.

The numerical values of β resulted from the solution procedures described in the previous section. Note the stiffnesses of these various geometries differ by at most 3%. It should be of interest in foundation design that the bearing stiffness of a footing is approximately independent of the shape if the area is fixed. This is similar to the previous result for uniform

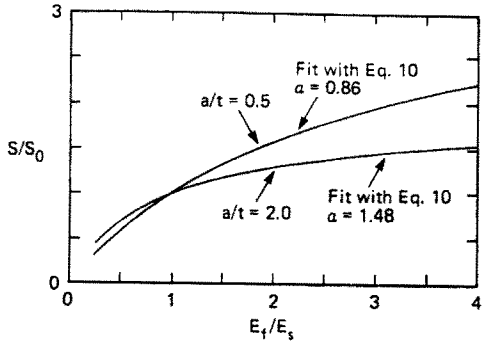

Fig. 6. Results of fitting eqn (10) to the curves in Fig. 5.

bearing load on rectangular regions of various aspect ratios on a half-space[3]: the stiffness differs significantly from that for a square region only when the aspect ratio exceeds two. For indentation testing this means that use of eqn (1) to calculate Young's modulus for a bulk sample will cause at most an error of 3% for Triangular or Vicker's indenters.

The effect of indenter shape is more pronounced when a film is present on the substrate. Results are presented for the circular, square, and triangular punches in Figs 3–5, for $\nu_f = \nu_s = \nu_0 = 0.3$ and $E_0/E_s = 8$. The results are only weakly dependent on Poisson's ratio. The value chosen for E_0/E_s is realistic, for example, for a diamond indenter and silicon substrate. The ordinates are normalized to the results for a substrate with no layer, and a family of curves of stiffness as a function of E_f/E_s is obtained for various a/t where $a = \sqrt{A}$ and t is the film thickness. The family is bracketed by the limits as $a/t \to \infty$ and $a/t \to 0$. In the former case, the film is vanishingly thin and has no effect so a horizontal line through $S/S_0 = 1$ is obtained. In the latter case of very thick films the film elastic properties dominate and the asymptotic limit is

$$S/S_0 = \frac{(1-\nu_s^2)/E_s + (1-\nu_0^2)/E_0}{(1-\nu_f^2)/E_f + (1-\nu_0^2)/E_0}.$$

It is reasonable to expect a smooth transition between these limits, which is the justification for the parameterization in eqn (2), suggested in Ref.[1]. Based on eqn (2), the result for S/S_0 is

$$S/S_0 = \frac{(1-\nu_s^2)/E_s + (1-\nu_0^2)/E_0}{(1-\nu_f^2)/E_f(1-e^{-\alpha t/a}) + (1-\nu_s^2)/E_s\, e^{-\alpha t/a} + (1-\nu_0^2)/E_0}. \tag{10}$$

Values of α were next determined to least-squares fit S/S_0 from eqn (10) to the curves in Figs 3–5. For all cases tested a good fit was provided. Two examples are shown in Fig. 6 for a triangular punch; in both these examples the fitted curve based on eqn (10) is indistinguishable from the numerical curve. The values of α were found to be dependent on a/t, as shown in Fig. 7. The values for the triangular and square punches were similar but α for the circular punch is quite different. This is because S/S_0 for the triangular and square punches is similar (Figs 4 and 5) but somewhat different for the circular punch (Fig. 3), and α is sensitive to the small changes in the curves in Figs 3–5. An empirically determined value of 0.25 was presented for α in Ref. [1], based on indentation testing of tungsten films on a silicon substrate. Equation 2 was based on h/t instead of a/t in Ref. [1]. The measured depth results in Ref. [1] were already corrected for the non-ideal indenter shape, so the results may be expressed in terms of a/t by using the relation for an ideal pyramidical indenter geometry, $a = 4.95h$. The equivalent empirically determined value of α based on a/t is then 1.24. The data presented in Ref. [1] on which the empirical determination of α was based covered a range of values of a/t, with an average value of a/t of 1.3. Using $a/t = 1.3$ and the least squares fitting procedure described above, an analytically determined value

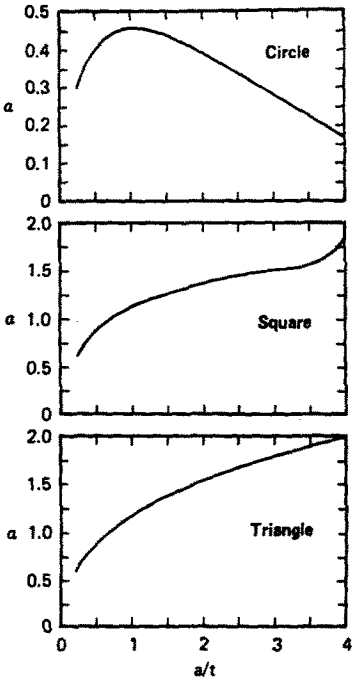

Fig. 7. Parameter α as a function of normalized punch size.

of 1.27 was obtained for α. This level of agreement with the theory presented here and previously reported experimental results is encouraging.

Empirical calibration of α in eqn (10) is a tedious process, and requires that a thin film with known elastic constants be deposited with thicknesses in the range of interest. This requires using a material such as tungsten the bulk values of which are well characterized and assuming that its film elastic properties do not differ from the bulk values. The necessity for this procedure is eliminated based on the theory presented herein.

To use the theory to calculate E_f from measured values of the unloading stiffness S, the suggested procedure is as follows: calculate S_0 with eqn (9) and the appropriate value of β for the punch geometry used based on known values of elastic properties of indenter and substrate materials. The ratio of S/S_0 can then be calculated, and the appropriate curve in Figs 3–5 is chosen based on the known value of a/t, from which E_f can be determined. It should be noted that the curves in Figs 3–5 are not quite universal, they will be somewhat dependent on the ratio of E_0/E_s. If the actual value of E_0/E_s differs from the value of eight used in producing Figs 3–5, then E_f should be solved for using eqn (10) and the appropriate value of α from Fig. 7. The value of α in eqn (10) was found to be independent of E_0/E_s.

REFERENCES

1. M. Doerner and W. Nix, A method for interpreting the data from depth-sensing indentation measurements. *J. Mater. Res.* **4**, 601 (1986).
2. J. Loubet, J. Georges, J. Marchesini and G. Meille, Vicker's indentation of magnesium oxide. *J. Tribology* **106**, 43 (1984).
3. S. Timoshenko and J. Goodier, *Theory of Elasticity*, 3rd Edn. McGraw-Hill, New York (1970).
4. W. Chen and P. Engel, Impact and contact stress analysis in multilayered media. *Int. J. Solids Structures* **8**, 1257 (1972).
5. R. King and T. O'Sullivan, Sliding contact stresses in a two-dimensional layered elastic half-space. *Int. J. Solids Structures* **23**, 581–597 (1987).
6. O. Zienkewicz, *The Finite Element Method*. McGraw-Hill, New York (1977).
7. D. Burmister, The general theory of stresses and displacements in layered systems. *J. Appl. Phys.* **16**, 89 (1945).
8. W. Chen, Computation of stresses and displacements in a layered elastic medium. *Int. J. Engng Sci.* **9**, 775 (1971).
9. G. Forsythe, M. Malcolm and C. Moler, *Computer Methods for Mathematical Computations*. Prentice-Hall, Englewood Cliffs, New Jersey (1977).

APPENDIX. SOLUTION FOR A UNIFORMLY LOADED RECTANGULAR REGION ON A LAYERED HALF-SPACE

As discussed in the text, numerical quadrature to obtain displacements is inaccurate at small r because the "Green's function" $G(r)$ becomes singular. This is alleviated by evaluating the superposition integral in closed form for small r. $G(r)$ for a half-space is given by the Boussinesq solution which is proportional to $1/r$. This is approached for very small r for the layered half-space. For somewhat larger r where the presence of the substrate is not totally negligible it is reasonable to approximate $G(r)$ by the same functional form with a different proportionality constant. Thus $G(r) \sim c/r$ where c is determined by least-squares fitting to the numerical evaluated expression for the layered half-space for small r. The solution for a uniform pressure p_0 on a rectangle of width $2a$ and length $2b$ on a layered half-space for small r is then given by

$$w(x, y) = \int_{-a}^{a} \int_{-b}^{b} c/\sqrt{((x-\xi)^2+(y-\eta)^2)}\, d\xi\, d\eta.$$

This is a surprisingly tedious integral to evaluate. The result is

$$w(x, y) = p_0 c \left\{ \eta \ln \left[\frac{f(a_1, \eta)}{f(a_2, \eta)} \right] + a_1/2 \ln \left[\frac{f(\eta, a_1) f(-\eta, a_2)}{f(-\eta, a_1) f(\eta, a_2)} \right] \right\} \Bigg|_{\eta=b_2}^{\eta=b_1}$$

where $f(u, v) = u+\sqrt{(u^2+v^2)}$, $a_1 = a-x$, $a_2 = -a-x$, $b_1 = b-y$, and $b_2 = -b-y$.